

The viability of the 3+1 neutrino model in the supernova neutrino process

Heamin Ko,¹ Dukjae Jang,^{1,*} Motohiko Kusakabe,² and Myung-Ki Cheoun¹

¹*Department of Physics and OMEG Institute, Soongsil University, Seoul 06978, Republic of Korea*

²*School of Physics and International Research Center for Big-Bang Cosmology and Element Genesis, Beihang University, Beijing 100083, China*

(Dated: January 26, 2022)

Adopting the 3+1 neutrino mixing parameters by the IceCube and shortbase line experiments, we investigate the sterile-active neutrino oscillation effects on the supernova neutrino process. For the sterile neutrino (ν_s), we study two different luminosity models. First, we presume that the ν_s does not interact with other particles through the standard interactions apart from the oscillation with the active neutrinos. Second, we consider that ν_s can be directly produced by ν_e scattering with matter. In both cases, we find that the pattern of neutrino oscillations can be changed drastically by the ν_s in supernova environments. Especially multiple resonances occur, and consequently affect thermal neutrino-induced reaction rates. As a result, ${}^7\text{Li}$, ${}^7\text{Be}$, ${}^{11}\text{B}$, ${}^{11}\text{C}$, ${}^{92}\text{Nb}$, ${}^{98}\text{Tc}$ and ${}^{138}\text{La}$ yields in the ν -process are changed. Among those nuclei, ${}^7\text{Li}$ and ${}^{11}\text{B}$ yields can be constrained by the analysis of observed SiC X grains. Based on the meteoritic data, we conclude that the second model can be allowed while first model is excluded. The viability of the second model depends on the sterile neutrino temperature and the neutrino mass hierarchy.

PACS numbers: 97.60.Bw, 14.60.St

Neutrino physics has become a new sight of the astrophysics. Beginning with observations of neutrinos from supernova (SN) 1987A [1], various neutrino properties have aroused lots of intensive discussions in astrophysics as well as particle and nuclear physics. In particular, the discovery of the neutrino oscillation is one of the most outstanding achievements in the modern physics [2, 3].

However, still the unexplained remains; neutrino anomalies have been reported, which are not partly in accord with the 3 neutrino model [4–7]. Although some ambiguities related to nuclear physics in reactors are being intensively investigated in theoretical and experimental sides [8–10], the inactive fourth flavor neutrino called “sterile neutrino (ν_s)” is still intriguing as one of possibilities to explain the anomalies and some other peculiar phenomena related to neutrinos [11].

Astrophysics studies on big bang nucleosynthesis [12–15] and X-ray observations from galaxy clusters [16–19] constrain the properties of ν_s and propose it as a dark matter candidate. In addition, SN studies found that the ν_s can enhance the SN explosion energy using the constraints on the mixing parameter from the X-ray astronomy [20]. Furthermore, it is investigated that active-sterile (ν_a - ν_s) flavor conversion in core-collapse SN leads to enhancing the r-process elements so as to coincide with the observation of the metal-poor star HD 122563 [21].

Although the astrophysical phenomena leave a room for a possible existence of ν_s , IceCube experiments exclude a parameter region for the mixing between ν_s and ν_μ indicated by shortbase line (SBL) experiments, by showing no evidence of the anomalous ν_μ -disappearance [22]. In the analysis, IceCube collaborations assumed $\theta_{14} = \theta_{34} = 0$ to take into account the ν_μ disappearance, whereas the condition of $\sin^2 2\theta_{\mu e} \neq 0$ in SBL anomalies requires the $\theta_{14} \neq 0$. By improving the inconsistency,

a recent work finds a new global fitted mixing parameters of the 3+1 neutrino model as $\Delta m_{41}^2 \approx 1.75 \text{ eV}^2$, $\theta_{14} = 9.44^\circ$, $\theta_{24} = 6.93^\circ$ and $\theta_{34} = 0$ [23]. In this letter, we adopt those results to study the effects of ν_a - ν_s neutrino oscillation on the SN neutrino process (ν -process).

Despite the small cross section between neutrinos and nuclei, the ν -process turns out to be important to explore origin of some rare nuclei. For instance, the neutrino-induced nucleosynthesis in SN significantly affects abundances of light-to-heavy nuclei such as ${}^7\text{Li}$, ${}^{11}\text{B}$, ${}^{92}\text{Nb}$, ${}^{98}\text{Tc}$, ${}^{138}\text{La}$ and ${}^{180}\text{Ta}$ [24–26]. In order to include the ν_s in the ν -process in SN, we apply the 3+1 neutrino model and evaluate their viability. As a source of ν_s s, we consider two models for production mechanism [27]. First, we assume the non-interacting ν_s s produced only by mixing with ν_a s. Second, ν_s s can be directly created by electron neutrino collisions with matter.

One of the most important physical inputs in the ν -process is how to describe the neutrino oscillation behavior in SN environments. Generally, the time evolution of the 3+1 neutrino model is expressed as the following Schrödinger-like equation

$$i \frac{d}{dt} \begin{pmatrix} \nu_e \\ \nu_\mu \\ \nu_\tau \\ \nu_s \end{pmatrix} = \hat{H} \begin{pmatrix} \nu_e \\ \nu_\mu \\ \nu_\tau \\ \nu_s \end{pmatrix}, \quad (1)$$

where we use units of $\hbar = c \equiv 1$. For the non-interacting ν_s , we compose the total Hamiltonian as vacuum (\hat{H}_{vacuum}) and matter (\hat{H}_{matter}) terms,

$$\hat{H}_{\text{vacuum}} = U \text{diag}(0, \frac{\Delta m_{21}^2}{2E_\nu}, \frac{\Delta m_{31}^2}{2E_\nu}, \frac{\Delta m_{41}^2}{2E_\nu}) U^\dagger, \quad (2)$$

$$\hat{H}_{\text{matter}} = \text{diag}(V_{\text{CC}} + V_{\text{NC}}, V_{\text{NC}}, V_{\text{NC}}, 0),$$

where U and E_ν , respectively, denote the 4×4 unitary mixing matrix [23] and neutrino energy. The mass squared difference is defined as $\Delta m_{ij}^2 \equiv m_i^2 - m_j^2$. Mixing parameters for three active flavors are adopted from the Particle Data Group [28]. Mass eigenstates are composed of the highest fourth mass state dominated by the ν_s [23] and others for three $\nu_{\alpha s}$ whose mass hierarchy (MH) has two possible cases known as normal and inverted hierarchies (NH and IH). In the non-interacting ν_s model, the fourth diagonal term in \hat{H}_{matter} would be zero while other terms for active flavors are given as charged and neutral current potentials (V_{CC} and V_{NC}). Note that the fourth term can also be neglected for the second model since the interaction strength of ν_s is constrained to be weak enough [27, 29].

With the 3+1 neutrino model, we investigate the SN ν -process up to the He layer with Lagrange mass coordinate ranging from $1.6 M_\odot$ to $6 M_\odot$, which is based on SN1987A model with the metallicity in Large Magellanic Cloud (LMC) *i.e.* $Z = 1/4 Z_\odot$. We use an explosion energy of 10^{51} erg and a hydrodynamical model in Ref. [30] based on the public code, blcode [31]. The reaction network and thermal nuclear reactions rates are, respectively, taken from Ref. [30] and JINA data base [32]. For cross sections of neutrino-induced reactions, those for ^4He and ^{12}C are adopted from Ref. [33]; those for intermediate nuclei of ^{12}C to ^{80}Kr from [34]; those for heavy elements related to production of ^{92}Nb , ^{98}Tc , ^{138}La and ^{180}Ta from [35, 36].

Figure 1 shows the survival probability of ν_e in SN explosion with the 3+1 neutrino model. For the NH case (left-upper panel), we find three kinds of resonances resulting from the Mikheyev–Smirnov–Wolfenstein effect [40, 41]. For the resonance condition, the larger the mass squared difference is, the higher matter density is required. Therefore, the conversion between ν_e and ν_s occurs in the first resonance region at $M_r \sim 1.6 M_\odot$ since Δm_{41}^2 is the largest and the 4th mass state is dominantly occupied by ν_s . Note that this resonance region is moved to inner side when sterile neutrino is heavier, but the neutrino process is not significantly affected by this change. The second resonance follows in the regions of $3 M_\odot < M_r < 3.5 M_\odot$, where ν_μ converts to ν_e by the similar condition. In the case of the IH, the conversion between the ν_s and ν_e also occurs in the similar region. The difference is in the outer region where the probability $P_{\nu_s \nu_e}$ survives instead of $P_{\nu_\tau \nu_e}$ value in NH.

The oscillation probability largely affects the neutrino-induced reaction rates. For the 3+1 neutrino model, the neutrino reaction rate can be written as

$$\lambda(t, r; T_{\nu_\beta}) = \frac{1}{4\pi r^2} \sum_{\alpha, \beta = e, \mu, \tau, s} \frac{\mathcal{L}_{\nu_\beta}(t)}{\langle E_{\nu_\beta} \rangle} \langle \sigma_{\nu_\alpha} P_{\nu_\beta \nu_\alpha}(r; T_{\nu_\beta}) \rangle \quad (3)$$

where r is the radius from the center of proto-neutron star. $\langle E_{\nu_\beta} \rangle$ and $\langle \sigma_{\nu_\alpha} P_{\nu_\beta \nu_\alpha} \rangle$, respectively, denote the

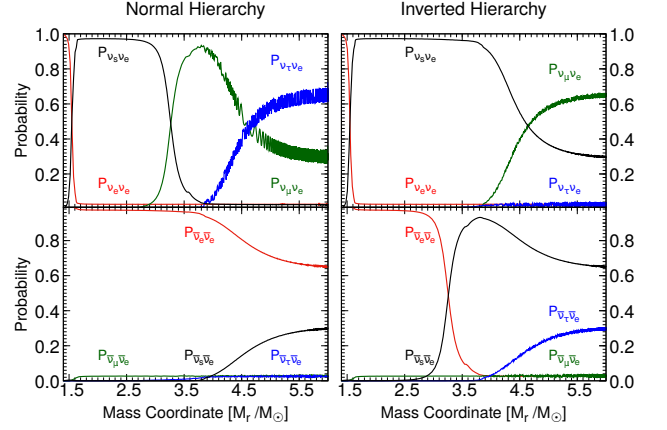


FIG. 1. Survival probability of ν_e with $E_\nu = 15$ MeV as a function of mass coordinate. $P_{\nu_\alpha \nu_e}$ denotes the flavor change probability from α to e flavor. Left and right panels show results for the NH and IH, respectively. Upper and lower panels, respectively, describe the probability $P_{\nu_\alpha \nu_e}$ for neutrinos and anti-neutrinos.

thermally averaged energy and the averaged cross section multiplied by the flavor change probability with Fermi-Dirac distribution for neutrino temperature T_{ν_β} used in Ref. [26]. \mathcal{L}_{ν_β} stands for the luminosity of the ν_β determined by initial conditions.

In general, the \mathcal{L}_{ν_s} depends on their production rate, which is determined by the oscillation probability ($P_{\nu_\alpha \nu_s}$) for the non-interacting ν_s . Near the SN core, the high baryon density ($\rho_B \sim 10^{14} \text{g/cm}^3$) strongly suppresses the probability $P_{\nu_\alpha \nu_s}$, and \mathcal{L}_{ν_s} is feeble in comparison with \mathcal{L}_{ν_α} . Hence, in the first model, we set the initial \mathcal{L}_{ν_s} to zero (termed as null \mathcal{L}_{ν_s} model), while \mathcal{L}_{ν_α} is the same as the 3 neutrino model [37]. Recent calculation of the \mathcal{L}_{ν_α} by ν -transport simulation [38] may affect the reaction rate, but the neutrino oscillation behavior is changed rarely.

Figure 2 shows nuclear abundances of light-to-heavy elements produced by SN ν -process with the 3 and the 3+1 neutrino model by using the null \mathcal{L}_{ν_s} model. The heavy nuclei such as ^{92}Nb , ^{98}Tc and ^{138}La are mainly produced at $1.5 M_\odot < M_r < 3.5 M_\odot$. In this region, regardless of MH, the conversion of $\nu_e \rightleftharpoons \nu_s$ suppresses the flux of ν_e because of the null \mathcal{L}_{ν_s} condition. The suppression of ν_e reduces the rates of the main reactions $^{92}\text{Zr}(\nu_e, e^-)^{92}\text{Nb}$, $^{98}\text{Mo}(\nu_e, e^-)^{98}\text{Tc}$ and $^{138}\text{Ba}(\nu_e, e^-)^{138}\text{La}$. Consequently, mass fractions of the heavy nuclei are decreased in this model. In the region of $M_r > 3.5 M_\odot$, on the other hand, abundances of heavy elements in the 3+1 neutrino model of IH case are smaller than those by the NH and 3 neutrino model. This result comes from the incomplete recovery of ν_e in the outer region (Fig. 1). ν_μ and ν_τ cannot sufficiently replenish the ν_e flux in the outer region in the IH case, although the flavor change to ν_e occurs at $M_r \gtrsim 4 M_\odot$. Therefore, unlike the 3 neutrino model,

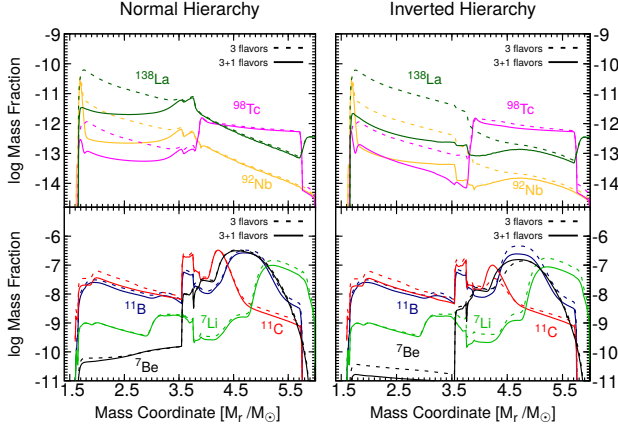


FIG. 2. Mass fractions of ${}^7\text{Li}$, ${}^7\text{Be}$, ${}^{11}\text{B}$, ${}^{11}\text{C}$, ${}^{92}\text{Nb}$, ${}^{98}\text{Tc}$ and ${}^{138}\text{La}$ as a function of the mass coordinate after 50 seconds from SN explosion. Left and right panels, respectively, correspond to the NH and IH cases. Dashed and solid lines denote the results in the 3 and the 3+1 neutrino model with the null \mathcal{L}_{ν_s} model, respectively.

total abundances of heavy elements in the 3+1 neutrino model depend on the neutrino MH.

In the outer region, the different oscillation patterns between NH and IH significantly affect light elements abundances (lower panels in Fig. 2). For the NH case, the suppression of $\bar{\nu}_e$ by $\bar{\nu}_s$ reduces the ${}^7\text{Li}$ abundance because of a decreased rate of ${}^4\text{He}(\bar{\nu}_e, e^+n){}^3\text{H}(\alpha, \gamma){}^7\text{Li}$. For the IH case, on the other hand, the reaction ${}^4\text{He}(\nu_e, e^-p){}^3\text{He}$ as well as ${}^4\text{He}(\bar{\nu}_e, e^+n){}^3\text{H}$ is hindered by a suppressed flux of ν_e . Thus, the reduced fluxes of ν_e and $\bar{\nu}_e$ result in significantly fewer ${}^3\text{H}$ and ${}^3\text{He}$ (compared with those in the 3 neutrino model [30]). This leads to reduced final abundances of ${}^7\text{Li}$ and ${}^{11}\text{B}$ which are produced via radiative α capture reactions.

Table I shows the abundance ratio of ${}^7\text{Li}$ and ${}^{11}\text{B}$ by the null \mathcal{L}_{ν_s} model with the observational data from the bayesian analysis of SiC X grains. We assume that elements in SiC X grains are uniformly mixed before it condensed in the SN ejecta long before the solar system formation. With the assumption, we integrate the mass fractions of ${}^7\text{Li}$ and ${}^{11}\text{B}$ after the decay of unstable nuclei over the whole mass region. The analysis of SiC X grains constrains the ratio of ${}^7\text{Li}$ and ${}^{11}\text{B}$ produced by the neutrino process as ${}^7\text{Li}/{}^{11}\text{B} = -0.31 \pm 0.42$ [39]. Our results by the null \mathcal{L}_{ν_s} model demonstrate that the 3 neutrino model is only allowed in the IH case within the 3σ limit and the 3+1 neutrino model is excluded.

As the second model, we consider that ν_s s can be directly produced in ν_e collision with matter. In this case, the cross section for the ν_s production can be written as $\sigma(\nu_e X \rightarrow \nu_s X) = A\sigma_{eX}(\nu_e X \rightarrow \nu_e X)$, where X is an electron, neutron, or proton, and A is a parameter for the interaction strength. The cross section leads to the

ν model	NH	IH	Observation [39]
3 flavors	1.22	0.80	< 0.53 (2σ 95% C.L.)
3+1 flavors	1.27	1.04	< 0.95 (3σ 99.7% C.L.)

TABLE I. Abundance ratio of ${}^7\text{Li}$ and ${}^{11}\text{B}$ produced within the whole mass coordinate region in the null \mathcal{L}_{ν_s} model and observations from analysis of SiC X grains.

luminosity of ν_s as [27]

$$\mathcal{L}_{\nu_s} \simeq n_e n_{\nu_e} A \sigma_{ee} V \langle E \rangle, \quad (4)$$

where n_i is the number density of particle i , V is the volume of the core, and $\langle E \rangle$ is an average energy of the neutrino. According to Ref. [27], total neutrino luminosity of SN1987A puts the constraint $A \leq 10^{-10}$. When we choose the upper limit $A = 10^{-10}$ and the core temperature of $T_C = 50$ MeV, \mathcal{L}_{ν_s} becomes about 10^{51} erg/s, which can be comparable with \mathcal{L}_{ν_a} . If the \mathcal{L}_{ν_s} is not negligible in this way, energetic ν_a s converted from the ν_s s increase relevant neutrino reaction rates because earlier decoupling of feebly interacting ν_s s may result in a higher temperature of decoupled ν_s s. As a simple test, we assume that the ν_s has an equivalent luminosity with those of ν_a s, *i.e.*, $\mathcal{L}_{\nu_s} = \mathcal{L}_{\nu_a}/8$ (termed as an equivalent \mathcal{L}_{ν_s} model), where \mathcal{L}_{ν_a} is the total neutrino luminosity given as 10^{53} erg/s. Also, we set the temperature of the ν_s (T_{ν_s}) as a free parameter. The exact \mathcal{L}_{ν_s} and temperature should be derived by treating the decoupling process of ν_s s with the Boltzmann equation. It is, however, beyond the scope of the present paper.

In this equivalent luminosity model, the higher temperature the ν_s has, the more energetic ν_a s are produced by the neutrino oscillation. The energetic neutrinos enhance the neutrino reaction rates in Eq. (3). As a result, abundances of the heavy nuclei, *i.e.*, ${}^{92}\text{Nb}$, ${}^{98}\text{Tc}$ and ${}^{138}\text{La}$, are increased, contrary to the trend in Fig. 2 for the null \mathcal{L}_{ν_s} model.

Table II shows the ${}^7\text{Li}/{}^{11}\text{B}$ ratio with the equivalent \mathcal{L}_{ν_s} model. In the NH case, the conversion of ν_s s ($\bar{\nu}_s$ s) with high temperature enhances rates of ${}^4\text{He}(\bar{\nu}_e, e^+n){}^3\text{H}$ and ${}^4\text{He}(\nu, \nu'p){}^3\text{H}$, which leads to an increased ${}^{11}\text{B}$ abundance. On the other hand, the final ${}^7\text{Li}$ yield is predominantly contributed by the ${}^7\text{Be}$ produced via ${}^4\text{He}(\nu_e, e^-p){}^3\text{He}(\alpha, \gamma){}^7\text{Be}$ and ${}^4\text{He}(\nu, \nu'n){}^3\text{He}(\alpha, \gamma){}^7\text{Be}$. While the ν_e reaction rates are not significantly increased in the NH case, ν_e s produced by ν_s s in the IH case enhance the ν_e reaction rates. Besides, in the IH case, more $\bar{\nu}_e$ s converted from $\bar{\nu}_s$ s also contribute to the increase of the ${}^7\text{Li}$ abundance. Therefore, the ${}^7\text{Li}/{}^{11}\text{B}$ ratio is smaller in the NH case and larger in the IH case for higher ν_s temperatures.

The analysis data from SiC X allows both MHs in the 3+1 neutrino model within the 3σ limit for $T_{\nu_s} = 7$ MeV, whereas the only NH case is allowed for $T_{\nu_s} \geq 8$ MeV. When we consider that the typical core temperature of

Neutrino Mass Hierarchy	Temperature of ν_s			
	7 MeV	8 MeV	9 MeV	10 MeV
NH	0.88	0.82	0.78	0.78
IH	0.92	1.02	1.15	1.15

TABLE II. Total abundance ratio of ${}^7\text{Li}$ and ${}^{11}\text{B}$ in the 3+1 neutrino model with the equivalent luminosity of all flavors.

proto-neutron stars is about 50 MeV, ν_s s can carry much higher temperature than the highest adopted value in our calculation. Therefore, we can expect that the SiC X analysis may exclude the IH case of this model.

In summary, the present work investigates the viability of the 3+1 neutrino model in the SN ν -process adopting the global fitting data of IceCube and SBL experiments. For the 3+1 neutrino model, two luminosity models are investigated. First, for the non-interacting ν_s s, it is unlikely to produce the ν_s s in the inner region due to the small mixing, so we assume the null \mathcal{L}_{ν_s} . The flavor change from ν_e to ν_s reduces neutrino reaction rates in the SN ν -process, and the SiC X analysis excludes the 3+1 neutrino model at the 3σ level. Second, we take the equivalent luminosity for all flavors. In that case, the neutrino oscillation enhances neutrino reaction rates due to the high temperature of decoupled ν_s s. Comparing our result with the SiC X analysis, it is shown that the 3+1 neutrino model is only allowed at $T_{\nu_s} = 7$ MeV in the IH case within the 3σ limit, while the NH case is fully allowed. Even though we regard T_{ν_s} as the free parameter in this calculation, it is important to estimate the T_{ν_s} and \mathcal{L}_{ν_s} in the SN explosion based upon an accurate kinetic theory for the neutrino transport. We expect that future study on the decoupling process of ν_s s would suggest a clue for the existence of ν_s s as well as the neutrino MH.

This work of H.K., D.J. and M.-K.C. was supported by Korea National Research Foundation of Korea (Grants No. 2013M7A1A10757b4 and No. NRF-2017R1E1A1A01074023). The work of M.K. was supported by NSFC Research Fund for International Young Scientists (11850410441).

* havevirtue@ssu.ac.kr

[1] K. Hirata *et al.* [Kamiokande-II Collaboration], Phys. Rev. Lett. **58**, 1490 (1987).
[2] T. Kajita, Rev. Mod. Phys. **88**, no. 3, 030501 (2016).
[3] A. B. McDonald, Rev. Mod. Phys. **88**, no. 3, 030502 (2016).
[4] A. Aguilar-Arevalo *et al.* [LSND Collaboration], Phys. Rev. D **64**, 112007 (2001).
[5] A. A. Aguilar-Arevalo *et al.* [MiniBooNE Collaboration], Phys. Rev. Lett. **105**, 181801 (2010).
[6] B. Bhattacharya, R. J. Hill and G. Paz, Phys. Rev. D **84**, 073006 (2011).

[7] C. Giunti and M. Laveder, Phys. Rev. C **83**, 065504 (2011).
[8] D. A. Dwyer and T. J. Langford, Phys. Rev. Lett. **114**, no. 1, 012502 (2015).
[9] J. Ashenfelter *et al.* [PROSPECT Collaboration], Phys. Rev. Lett. **121**, no. 25, 251802 (2018).
[10] J. Petkovi, T. Marketin, G. Martinez-Pinedo and N. Paar, J. Phys. G **46**, no. 8, 085103 (2019).
[11] A. Boyarsky, M. Drewes, T. Lasserre, S. Mertens and O. Ruchayskiy, Prog. Part. Nucl. Phys. **104**, 1 (2019).
[12] M. Archidiacono, N. Fornengo, C. Giunti, S. Hannestad and A. Melchiorri, Phys. Rev. D **87**, no. 12, 125034 (2013).
[13] J. Hamann, S. Hannestad, G. G. Raffelt, I. Tamborra and Y. Y. Y. Wong, Phys. Rev. Lett. **105**, 181301 (2010).
[14] G. Mangano and P. D. Serpico Phys. Lett. B **701**, 3, 296 (2011).
[15] D. Jang, M. Kusakabe and M. K. Cheoun, Phys. Rev. D **97**, no. 4, 043005 (2018).
[16] M. H. Chan and R. Ehrlich, Astrophys. Space Sci. **349**, 407 (2014).
[17] A. Boyarsky, A. Neronov, O. Ruchayskiy and M. Shaposhnikov, Phys. Rev. D **74**, 103506 (2006).
[18] A. Boyarsky, O. Ruchayskiy, D. Iakubovskiy and J. Franse, Phys. Rev. Lett. **113**, 251301 (2014).
[19] E. Bulbul, M. Markevitch, A. Foster, R. K. Smith, M. Loewenstein and S. W. Randall, Astrophys. J. **789**, 13 (2014).
[20] M. L. Warren, M. Meixner, G. Mathews, J. Hidaka and T. Kajino, Phys. Rev. D **90**, no. 10, 103007 (2014).
[21] M. R. Wu, T. Fischer, L. Huther, G. Martinez-Pinedo and Y. Z. Qian, Phys. Rev. D **89**, no. 6, 061303 (2014).
[22] M. G. Aartsen *et al.* [IceCube Collaboration], Phys. Rev. Lett. **117**, no. 7, 071801 (2016).
[23] G. H. Collin, C. A. Argelles, J. M. Conrad and M. H. Shaevitz, Phys. Rev. Lett. **117**, no. 22, 221801 (2016).
[24] S. E. Woosley, D. H. Hartmann, R. D. Hoffman and W. C. Haxton, Astrophys. J. **356**, 272 (1990).
[25] A. Heger, E. Kolbe, W. C. Haxton, K. Langanke, G. Martinez-Pinedo and S. E. Woosley, Phys. Lett. B **606**, 258 (2005).
[26] T. Hayakawa *et al.*, Phys. Rev. Lett. **121**, no. 10, 102701 (2018).
[27] E. W. Kolb, R. N. Mohapatra and V. L. Teplitz, Phys. Rev. Lett. **77**, 3066 (1996).
[28] K. A. Olive *et al.* [Particle Data Group], Chin. Phys. C **38**, 090001 (2014).
[29] R. Barbieri and R. N. Mohapatra, Phys. Rev. D **39**, 1229 (1989).
[30] M. Kusakabe *et al.*, Astrophys. J. **872**, no. 2, 164 (2019).
[31] C. Ott, V. Morozova and A. L. Piro <https://stellarcollapse.org/snec>.
[32] R. H. Cyburt *et al.*, Astrophys. J. Suppl. **189**, no. 1, 240 (2010).
[33] T. Yoshida, T. Suzuki, S. Chiba, T. Kajino, H. Yokomakura, K. Kimura, A. Takamura and D. H. Hartmann, Astrophys. J. **686**, 448 (2008).
[34] R. D. Hoffman and S. E. Woosley, Online database of Stellar Nucleosynthesis Data by Hoffmann and Woosley, <http://dbserv.pnpi.spb.ru/elbib/tablisot/toi98/www/astro/hw>.
[35] M. K. Cheoun, E. Ha, T. Hayakawa, T. Kajino and S. Chiba, Phys. Rev. C **82**, 035504 (2010).
[36] M. K. Cheoun, E. Ha, T. Hayakawa, S. Chiba, K. Naka-

- mura, T. Kajino and G. J. Mathews, Phys. Rev. C **85**, 065807 (2012).
- [37] T. Yoshida, T. Kajino and D. H. Hartmann, Phys. Rev. Lett. **94**, 231101 (2005).
- [38] E. O'Connor *et al.*, J. Phys. G **45**, no. 10, 104001 (2018).
- [39] G. J. Mathews, T. Kajino, W. Aoki, W. Fujiya and J. B. Pitts, Phys. Rev. D **85**, 105023 (2012).
- [40] L. Wolfenstein, Phys. Rev. D **17**, 2369 (1978).
- [41] S. P. Mikheyev and A. Y. Smirnov, Nuovo Cim. C **9**, 17 (1986).